Optical Sensing of L-dihydroxy-phenylalanine in Water by a High-affinity Molecular Receptor Involving a Cooperative Bind of Metal Coordination Bond and Boronate-Diol

María K. Salomón-Flores,[a] Alejandro O. Viviano-Posadas,[a] Josue Valdes-García,[a] Víctor López-Guerrero,[a] Diego Martínez-Otero,[ab] Joaquín Barroso-Flores,[ab] Juan M. German-Acacio,[c] Iván J. Bazany-Rodríguez,[d] and Alejandro Dorazco-González*[a]

[a] Institute of Chemistry, National Autonomous University of Mexico, Ciudad Universitaria, México, 04510, CDMX, México.
[b] Centro Conjunto de Investigación en Química Sustentable, UAEM-UNAM, Carretera Toluca-Atlacomulco Km 14.5, C. P. 50200, Toluca, Estado de México, México, Instituto de Química, Universidad Nacional Autónoma de México.
[c] Red de Apoyo a la Investigación, Coordinación de la Investigación Científica-UNAM, Instituto Nacional de Ciencias Médicas y Nutrición SZ, Ciudad de México, CP 14000, México
[d] Facultad de Química, Universidad Nacional Autónoma de México, Ciudad Universitaria CDMX, 04510 México.

Electronic Supporting Information

General Conditions:

Reagents and solvents were purchased as reagent grades and used without further purification.

2-acetylpiridine (Aldrich, 99%), potassium hydroxide (pellets, Tecsiquim, >85.0%), 4-isoquinolinecarboxaldehyde (Aldrich, 97%), 3-(bromomethyl)phenylboronic acid (Aldrich, 90%), ethanol (Tecqsiquim, >99.5%), acetonitrile (Tecsiquim, 99.5%), ammonium hydroxide solution (Aldrich, 29.50%), ethyl acetate (Aldrich, >99.5%), ethyl ether (Tecquisim, >99%), benzyl bromide (Aldrich, 98%), copper bromide (Aldrich, 99%), 3,4-dihydroxy-L-phenylalanine (Aldrich, >98%), L-tyrosine (Aldrich, >98%), epinephrine (Aldrich, >98%), dopamine (Aldrich, >98%), uronic acid (Aldrich, >98%), CD_3OD (Aldrich, >99%), dimethyl sulfoxide-d_6 (Aldrich, 99.5%), 3-(N-Morpholino)propanesulfonic acid, MOPS (Aldrich, 99.5%), sodium hydroxide (Tecsiquim, 97 %), deionized water. MOPS buffer solution (10 mM, pH 7.4) was prepared with deionized water. A stock solutions of corresponding Cu (II)-complex 1.0 mM, were made with acetonitrile.

Fluorescence and UV-Vis spectra were recorded on an Agilent Cary Eclipse fluorimeter and an Agilent Cary 100 spectrophotometer, respectively, both equipped with a thermostated cell holder at 25°C (±0.1). The source for Cary Eclipse was a 75W Xenon short arc lamp.

Fluorescence lifetime measurements: A Time Correlated Single Photon Counting (TCSPC) system coupled to a custom-built confocal microscope was used to acquire the fluorescence lifetimes. A 354 nm picosecond laser pulsed at 10 MHz (LDH-DC-405, PicoQuant) was focused into a 1 cm quartz cell with a 0.85 NA microscope objective. The fluorescence collected with the same objective passed through a 366 nm long-pass dichroic mirror (Chroma T510lpxrxt), a 364 nm notch filter (Chroma ZET405nf), and a 425 nm long pass emission filter (Chroma ET425lp) and was focused to an avalanche photodiode (PD-050-CTE, MPD). The laser controller (PDL-800-D, PicoQuant) and the APD were connected to a TCSPC card (PicoHarp 300, PicoQuant). The power of irradiation was controlled to obtain less than 1% of the detection events in order to avoid pile-up effects on the recorded histogram. Allura Red (analytical standard Sigma-Aldrich) was used to obtain the IRF under the same conditions of irradiation. All data were obtained and treated in SymphoTime 64 software (PicoQuant).[66]

^{1}H and ^{13}C NMR spectra were recorded on a Bruker Advance DPX 400 spectrometer at 400, 100 MHz respectively. ^{11}B NMR spectra were recorded on a Bruker Advance at 96 MHz and are reported in parts per million with respect to BF_3OEt_2 (δ=0).

High-Resolution Electrospray Ionization mass with positive scan spectra for FGH and **3Zn** were obtained with a Bruker Micro TOF II.

Electrospray Ionization mass spectrum with positive and negative scan for all synthesized molecules were obtained with a Waters CapLCcoupled Micromass Q-ToF Ultima ESI-instrument.

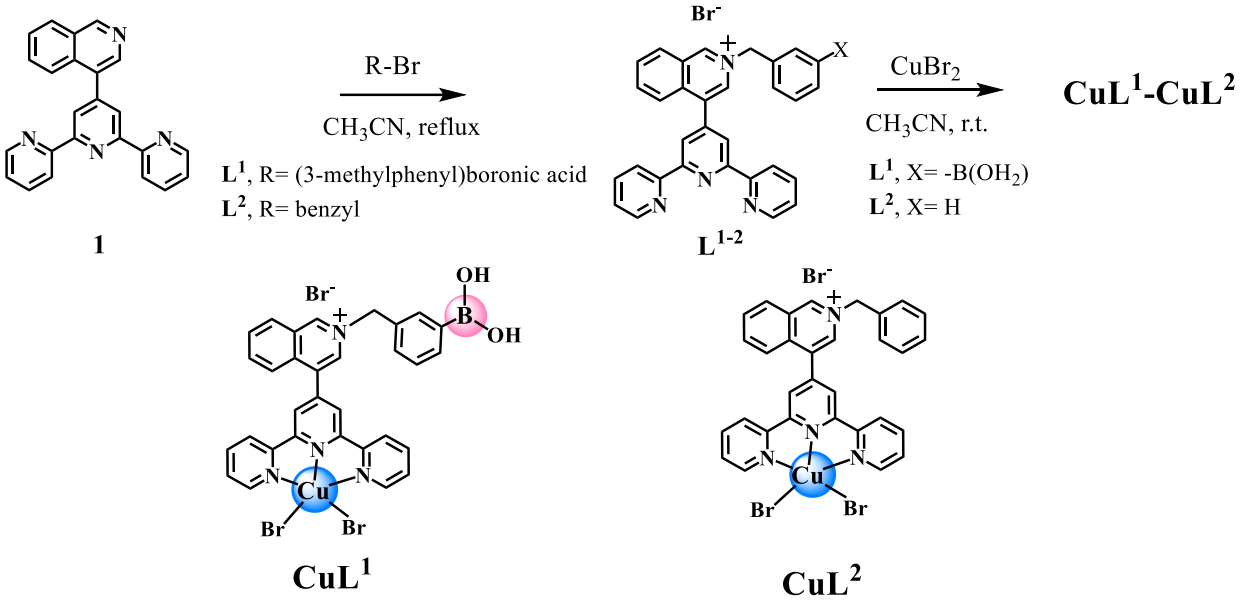

Scheme S1. Synthesis of Cu-complexes-based used in this work.

Chemical Synthesis

***Synthesis of compound* 1**: *4-([2,2':6',2''-terpyridin]-4'-yl)isoquinoline.* 2-acetylpyridine (250.3 mg, 232.0 µL, 2.04 mmol) was dissolved in an ethanolic solution (60.0 ml) of KOH (500.0 mg, 8.90 mmol) in a balloon flask and it was vigorously stirred for 10.0 min., separately, 4-isoquinolinecarboxaldehyde (164.01 mg, 1.04 mmol) was dissolved in EtOH (10.0 mL) and added drop by drop to the 2-acetylpyridine basic solution. The mixture reaction was stirred for ~ 20 min. at r. t., then, aqueous NH_3 (10.5 ml, 12.5 mmol, 29.50%) was added and refluxed for 48 h. under a N_2 atmosphere. The solvent was reduced under vacuum up to ~ 20 % of the initial volume and cold distilled water (100.0 mL) was added to give a precipitate. This precipitate was filtered off, washed with water twice (25.0 mL) and recrystallized in EtOH to obtain **1** as white crystalline powder. Yield: 242.0 mg (65.0 %).

^{1}H NMR (300 MHz, 25 °C, $CDCl_3$) δ 9.33 (s, 1H), 8.73 (dt, *J*= 7.99, 1.09 Hz, 2H), 8.69 (ddd, *J*= 4.80, 1.81, 0.93 Hz, 2H), 8.66 (s, 2H), 8.64 (s, 1H), 8.10-8.07 (m, 1H), 8.00-7.97 (m, 1H), 7.91 (td, *J*= 7.85 Hz, 7.75, 1.81 Hz, 2H), 7.74–7.68 (m, 2H), 7.36 (ddd, *J*= 7.50, 4.77, 1.22 Hz, 2H)

^{13}C NMR (75 MHz, 25 °C, $CDCl_3$) δ 155.97, 155.86, 153.06, 149.25, 147.23, 142.77, 136.93, 133.64, 131.30, 131.13, 128.31, 128.05, 127.47, 124.41, 123.99, 122.24, 121.42.

EI-MS (m/z): calculated for [$C_{24}H_{15}N_4^+$], 359.13; found, 359.00.

Synthesis of ligand L[1]*: 4'-[N-(3-boronobenzyl)-4-isoquinolinium] 2,2':6',2''-terpyridine bromide.* **1** (50.0 mg, 0.14 mmol) and 1.10 equiv of 3-(bromomethyl)phenylboronic acid (36.47 mg, 0.19 mmol) were dissolved in anhydrous CH_3CN (70 mL) and refluxed for 72 h with a N_2 atmosphere. Then, the solvent was removed under reduced pressure and ethyl acetate (40 mL) was added. The mixture was stirred for 5 h. Finally, the solid was filtered off, washed with Et_2O twice (5 mL) and dried under vacuum for ~ 3 h. to give **L1** as white powder. Yield: 71.82 mg, (90.0 %).

^{1}H NMR (301 MHz,25°C, DMSO-d_6) δ 10.39 (s, 1H), 9.19 (d, *J*=1.33 Hz, 1H), 8.76–8.69(m, 5H), 8.66 (s, 2H), 8.32-8.26 (m, 1H), 8.21-8.12 (m, 4H), 8.08 (td, *J*=7.72, 1.81 Hz, 2H), 7.97 (s, 1H), 7.84 (dt, *J*=7.39, 1.23 Hz, 1H), 7.69 (dt, *J*=7.82, 1.51 Hz, 1H), 7.55 (ddd, *J*=7.58, 4.77, 1.24 Hz, 2H), 7.43 (t, *J*=7.54 Hz, 1H), 6.07 (s, 2H).

^{13}C NMR (101 MHz, 25°C, DMSO-d_6) δ 155.77, 154.41, 150.21, 149.52, 143.34, 138.17, 137.82, 136.28, 135.22, 134.97, 134.57, 134.39, 133.35, 131.63, 131.53, 130.59, 128.60, 128.34, 127.90, 125.04, 124.83, 121.67, 121.24, 63.78.

HRMS-ESI$^+$ (*m/z*): calculated for $[C_{31}H_{24}BN_4O_2]^+$: 495.20, found: 495.20453. ATR-IR *v* (cm^{-1}): 3300(m), 2926(m), 1584(m), 1449(m), 1352(m), 1096–1030(m).

Synthesis of ligand L[2]*, 4'-[N-(benzyl)-4-isoquinolinium]-2,2':6',2''-terpyridine bromide*. **1** (50.0 mg, 0.14 mmol) and 10.0 equiv. of benzyl bromide (168.13.0 µL, 1.4 mmol) were dissolved in anhydrous CH_3CN (70 mL) and refluxed for 24 h. with a N_2 atmosphere. The solvent was removed under reduced pressure, ethyl acetate (40.0 mL) was added it was left stirring for ~ 5 h. at r.t. The solid was filtered under vacuum and crystallized in an EtOH-acetone (1:1, v/v) system, obtaining white needle-shaped crystals. Yield: 55.86 mg (70 %).

^{1}H NMR (300 MHz, 25 °C, DMSO-d_6) δ (ppm) 10.40 (s, 1H), 9.22 (s, 1H), 8.78–8.72 (m, 5H), 8.68 (s, 2H), 8.30 (ddd, *J*=8.41, 6.79, 1.34 Hz, 1H), 8.18 (dd, *J*=8.05, 1.13 Hz, 2H), 8.10 (td, *J*=7.73, 1.83 Hz, 2H), 7.68–7.65 (m, 2H), 7.57 (ddd, *J*=7.52, 4.76, 1.20 Hz, 2H), 7.49–7.42 (m, 3H), 6.07 (s, 2H).

^{13}C NMR (75 MHz, 25°C, DMSO-d_6) δ 155.61, 154.27, 150.19, 149.38, 143.31, 138.12, 137.88, 136.23, 135.18, 134.45, 134.30, 131.57, 131.47, 129.35, 129.20, 128.96, 127.84, 125.03, 124.76, 121.70, 121.26, 63.43. (two signals were not detected).

ESI$^+$-MS (*m/z*): calculated for $[C_{31}H_{23}N_4]^+$: 451.19, found: 452.351. ATR-IR *v* (cm^{-1}): 3035(m), 1584(m), 1399(m).

Table S1. Crystallographic data and structure refinement for **CuL^1** and **CuL^2**.

Crystal data	**CuL^1**	**CuL^2**
Empirical formula	$C_{33}H_{27}BBr_{2.54}Cl_{3.46}CuN_4O_2$	$C_{31}H_{29}Br_3CuN_4O_3$
Formula weight (g mol$^-$)	911.55	808.85
Temperature (K)	100(2)	100(2)
Wavelength	1.54178 Å	0.71073
Crystal system	Monoclinic	Monoclinic
Space group	$P2_1/n$	$P2_1/c$
a (Å)	10.4148(2)	17.1481(8)
b (Å)	13.5810(3)	14.9862(7)
c (Å)	25.1875(5)	12.3646(6)
α (°)	90	90
β (°).	99.6130(10)	107.1466(9)
γ = 90°.	90	90
Volume (Å^3)	3512.58(12)	3036.3(2)
Z	4	4
Density calculated (mg/m^3)	1.724	1.769
Absorption coefficient (mm^{-1})	6.987	4.707
F(000)	1803	1604
Crystal size (mm^3)	0.166 x 0.144 x 0.127	0.264 x 0.158 x 0.075
Theta range for data collection (°)	3.559 to 71.905	2.195 to 27.445
Index ranges	-12<=h<=12, 0<=k<=16, 0<=l<=31	-22<=h<=22, -19<=k<=19, -16<=l<=16
Reflections collected	6649	65302
Independent reflections	6649 [R(int) = ?]	6938 [R(int) = 0.0358]
Completeness to theta	67.679° 97.4 %	25.242° 100.0 %
Refinement method	Full-matrix least-squares on F^2	Full-matrix least-squares on F^2
Data / restraints / parameters	6649 / 4 / 434	6938 / 24 / 407
Goodness-of-fit on F^2	1.033	1.040
Final R indices [I>2sigma(I)]	R1 = 0.0489, wR2 = 0.1393	R1 = 0.0294, wR2 = 0.0759
R indices (all data)	R1 = 0.0541, wR2 = 0.1456	R1 = 0.0346, wR2 = 0.0789
Extinction coefficient	n/a	n/a
Largest diff. peak and hole (e.Å^{-3})	1.596 and -0.665	2.409 and -1.563

Table S2. Hydrogen Bonds for **CuL[1]** [Å and °].

D-H...A	d(D-H)	d(H...A)	d(D...A)	<(DHA)
O(1)-H(1)...Br(2)	0.852(17)	2.554(13)	3.358(3)	158(3)

Table S3. Hydrogen Bonds for **CuL[2]** [Å and °]

D-H...A	d(D-H)	d(H...A)	d(D...A)	<(DHA)
O(2)-H(2A)...Br(2)	0.834(10)	2.640(11)	3.471(2)	174(4)
O(2)-H(2B)...Br(2)#1	0.834(10)	2.585(16)	3.390(2)	162(4)
O(1)-H(1A)...Br(3)#2	0.843(10)	2.67(2)	3.477(3)	160(5)
O(1)-H(1B)...Br(3)#1	0.845(10)	2.716(17)	3.540(3)	165(5)
O(3^a)-H(3A^a)...O(2)	0.8401(10)	2.112(9)	2.915(7)	160(3)
O(3^a)-H(3B^a)...Br(3)	0.8400(11)	2.67(5)	3.400(7)	145(7)
O(3A^b)-H(3C^b)...O(2)	0.845(10)	2.107(9)	2.943(10)	170(7)
O(3A^b)-H(3D^b)...Br(3)	0.839(10)	2.55(6)	3.281(9)	147(10)

Symmetry transformations used to generate equivalent atoms:

#1 -x+1,-y+1,-z #2-x+1,y-1/2,-z+1/2

Table S4. Selected bond distances (Å) and angles (°) for boron and copper atoms in crystal **CuL[1]**.

1			
O(1)-B(1)	1.357(6)	N(1)-Cu(1)-N(2)	78.68(13)
O(2)-B1	1.361(6)	N(3)-Cu(1)-N(2)	157.25(13)
C(28)-B(1)	1.570(6)	N(1)-Cu(1)-Cl(4)	149.5(4)
O(1)-B(1)-O(2)	119.0(4)	N(3)-Cu(1)-Cl(4)	96.3(4)
O(1)-B(1)-C(28)	123.7(4)	N(2)-Cu(1)-Cl(4)	98.9(4)
O(2)-B(1)-C(28)	117.3(4)	N(1)-Cu(1)-Br(4)	149.80(16)
Br(1)-Cu(1)	2.5981(7)	N(3)-Cu(1)-Br(4)	97.75(15)
Br(4)-Cu(1)	2.375(3)	N(2)-Cu(1)-Br(4)	97.49(15)
Cl(4)-Cu(1)	2.138(9)	N(1)-Cu(1)-Br(1)	103.35(10)
Cu(1)-N(1)	1.956(3)	N(3)-Cu(1)-Br(1)	95.86(10)
Cu(1)-N(3)	2.042(3)	N(2)-Cu(1)-Br(1)	95.76(9)
Cu(1)-N(2)	2.051(3)	Cl(4)-Cu(1)-Br(1)	107.1(4)
N(1)-Cu(1)-N(3)	79.64(13)	Br(4)-Cu(1)-Br(1)	106.84(13)

Table S5. Selected bond distances (Å) and angles (°) for copper atom in crystal **CuL²**.

	2
Br(1)-Cu(1)	2.3580(4)
Br(2)-Cu(1)	2.6536(4)
Cu(1)-N(1)	1.951(2)
Cu(1)-N(2)	2.035(2)
Cu(1)-N(3)	2.044(2)
N(1)-Cu(1)-N(2)	79.52(8)
N(1)-Cu(1)-N(3)	79.38(8)
N(2)-Cu(1)-N(3)	156.29(8)
N(1)-Cu(1)-Br(1)	162.43(6)
N(2)-Cu(1)-Br(1)	98.52(6)
N(3)-Cu(1)-Br(1)	98.32(6)
N(1)-Cu(1)-Br(2)	93.82(6)
N(2)-Cu(1)-Br(2)	94.72(6)
N(3)-Cu(1)-Br(2)	97.35(6)
Br(1)-Cu(1)-Br(2)	103.749(13)

Table S6. Boronic acid-based molecular receptors for Levodopa.

Molecular receptor	**Signal**	**Apparent binding constant (M^{-1})**	**Media**	**Ref.**
Boronic acid appended Zn(II)-porphyrin	UV-vis	1.9×10^4	CH_3OH-H_2O	[1]
Boronic acid appended lucifer yellow dye	Turn-off	1.6×10^3	H_2O	[2]
Boronic acid appended quinoline derivative	Turn-off	1.4×10^3	H_2O	[3]
Boronic acid appended perylene derivative	UV-vis	3.2×10^4	H_2O	[4]
Boronic acid appended Zn(II)-terpy	Turn-off	1.0×10^6	H_2O	[5]
CuL¹	Tun-off	4.7×10^6	H_2O	This work

(1) Imada, T.; Kijima, H.; Takeuchi, M.; Shinkai, S. Selective Binding of Glucose-6-Phosphate, 3,4-Dihydroxyphenylalanine (DOPA) and Their Analogs with a Boronic-Acid-Appended Metalloporphyrin. *Tetrahedron* **1996**, *52* (8), 2817–2826. https://doi.org/https://doi.org/10.1016/0040-4020(96)00003-8.

(2) Coskun, A.; Akkaya, E. U. Three-Point Recognition and Selective Fluorescence Sensing of L-DOPA. *Org. Lett.* **2004**, *6* (18), 3107–3109. https://doi.org/10.1021/ol0488744.

(3) Wu, Z.; Yang, X.; Xu, W.; Wang, B.; Hao, F. A New Boronic Acid-Based Fluorescent Sensor for L-Dihydroxy-Phenylalanine. *Drug Discov. Ther.* **2011**, *6* (5), 238–241. https://doi.org/10.5582/ddt.2012.v6.5.238.

(4) Chen, X. X.; Wu, X.; Zhang, P.; Zhang, M.; Song, B. N.; Huang, Y. J.; Li, Z.; Jiang, Y. B. Multicomponent Covalent Dye Assembly for Tight Binding and Sensitive Sensing of L-DOPA. *Chem. Comm.* **2015**, *51* (71), 13630–13633. https://doi.org/10.1039/c5cc03495g.

(5) Iván J. Bazany-Rodríguez, María K. Salomón-Flores, Alejandro O. Viviano-Posadas, Marco A. García-Eleno, J. B.-F.; Diego Martínez-Oteroc and Alejandro Dorazco-González. Chemosensing of Neurotransmitters with Selectivity and Naked Eye Detection of L-DOPA Based on Fluorescent Zn(II)-Terpyridine Bearing Boronic Acid Complexes. *Dalt. Trans* **2021**, *50*, 4255–4269. https://doi.org/10.1039/d0dt04228e.

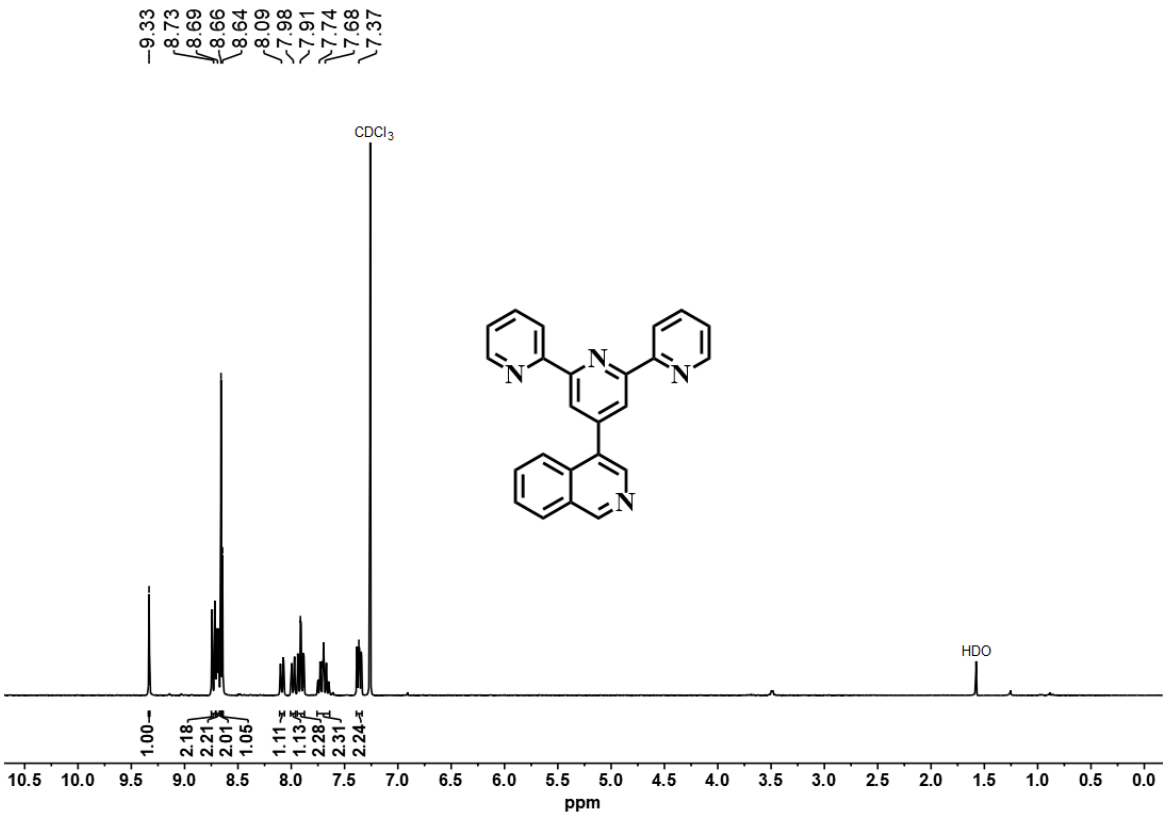

Fig. S1. ^{1}H NMR (300 MHz, 25°C) spectrum of **terpy-4-isoquinoline** in $CDCl_3$.

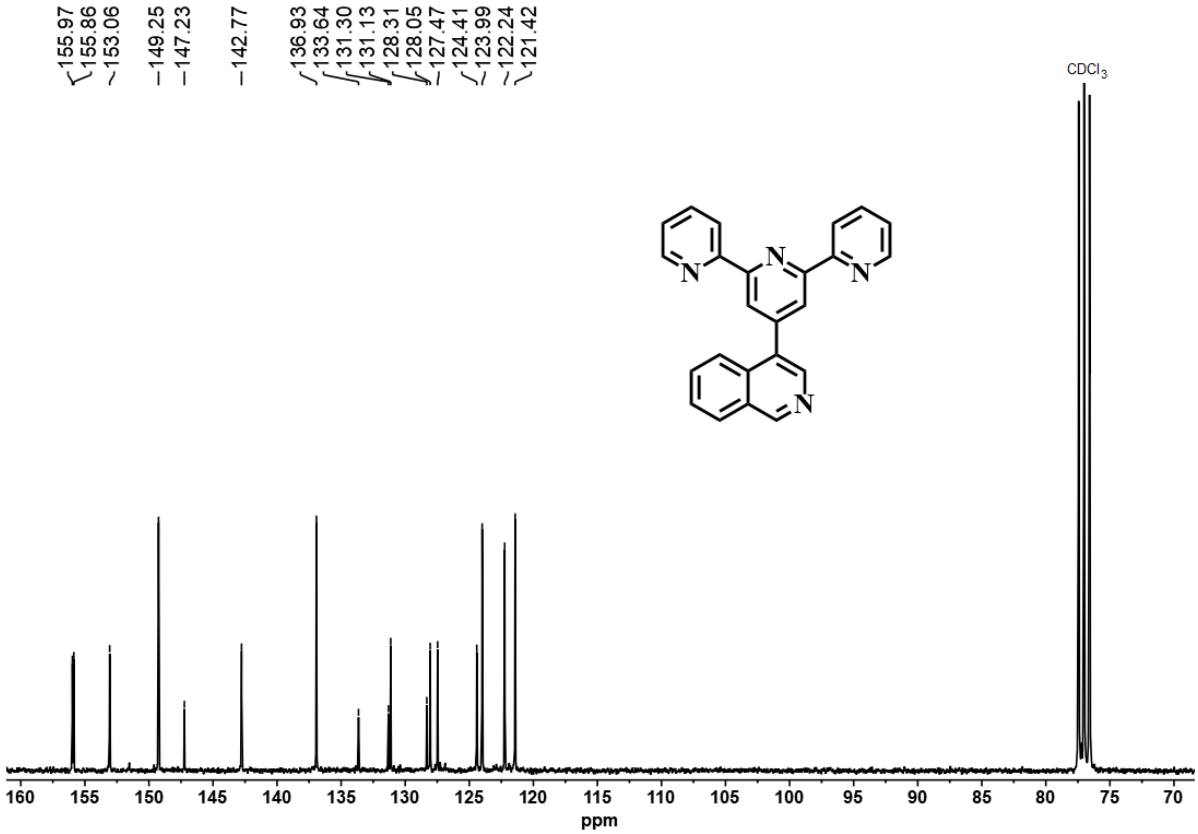

Fig. S2. ^{13}C NMR (75 MHz, 25°C) spectrum of **terpy-4-isoquinoline** in $CDCl_3$.

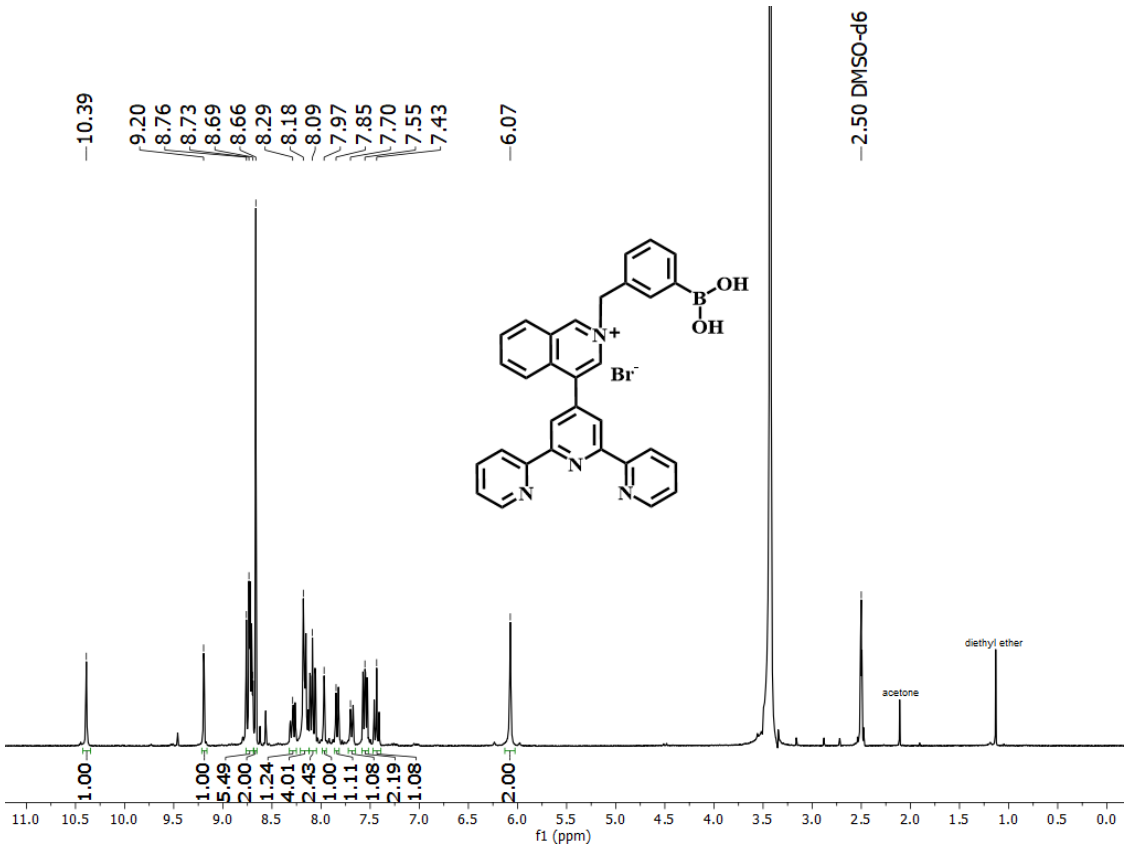

Fig. S3 ^{1}H NMR (300 MHz, 25°C) spectrum of **L^{1}** in DMSO-d_6.

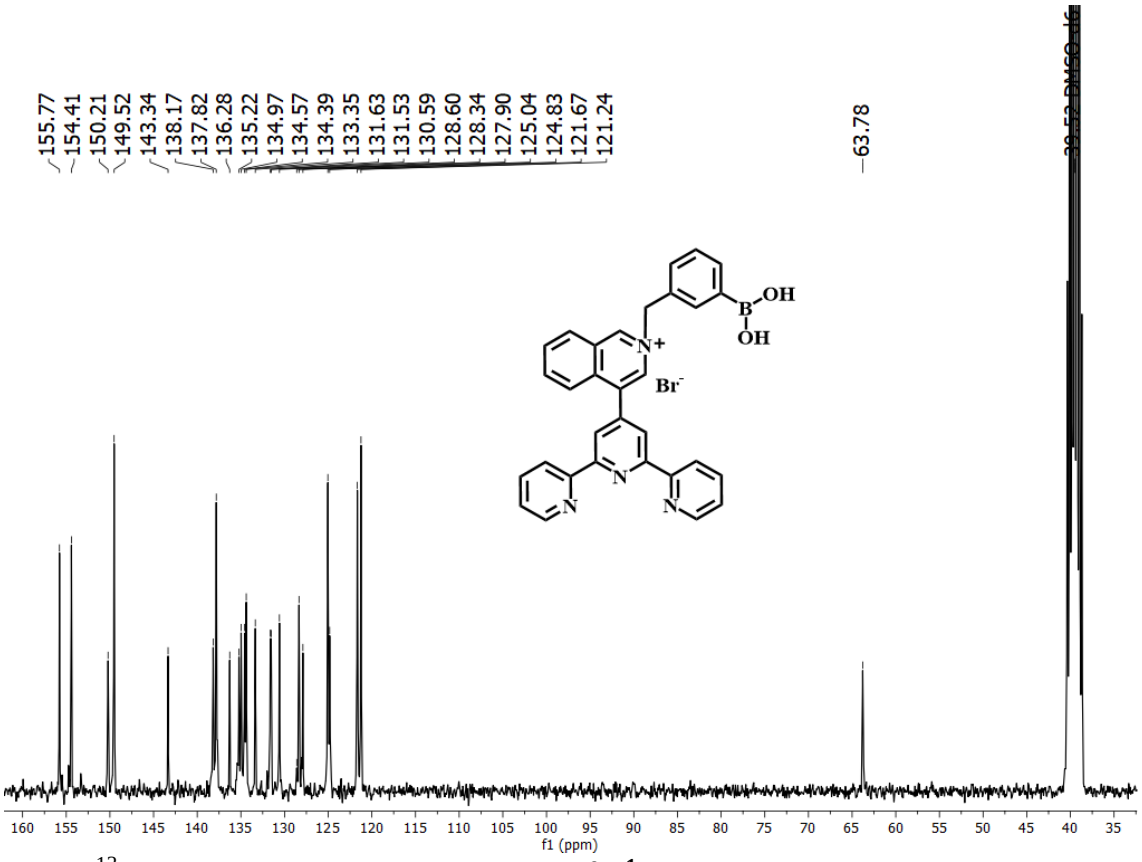

Fig. S4 ^{13}C NMR (75 MHz, 25°C) spectrum of **L^{1}** in DMSO-d_6.

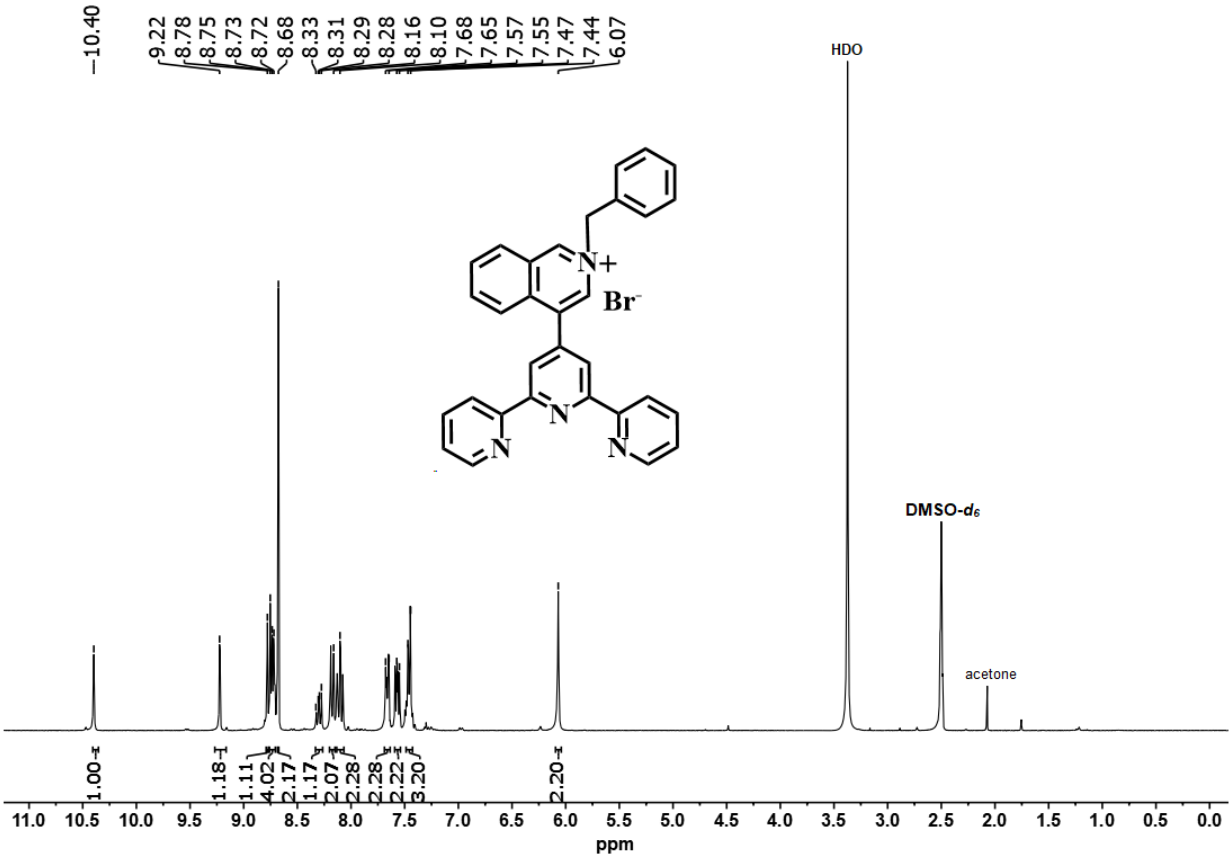

Fig. S5 ^{1}H NMR (300 MHz, 25°C) spectrum of **L²** in DMSO-d_6.

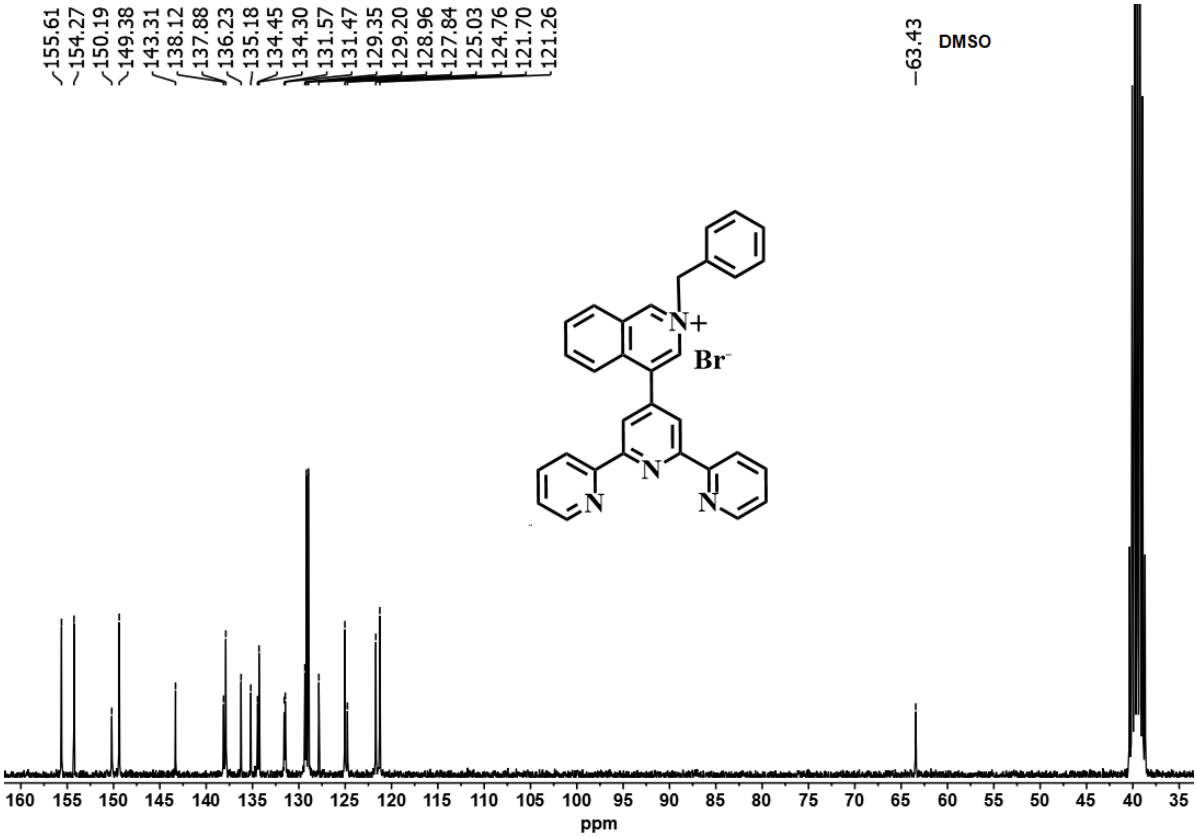

Fig. S6 ^{13}C NMR (75 MHz, 25°C) spectrum of **L²** in DMSO-d_6.

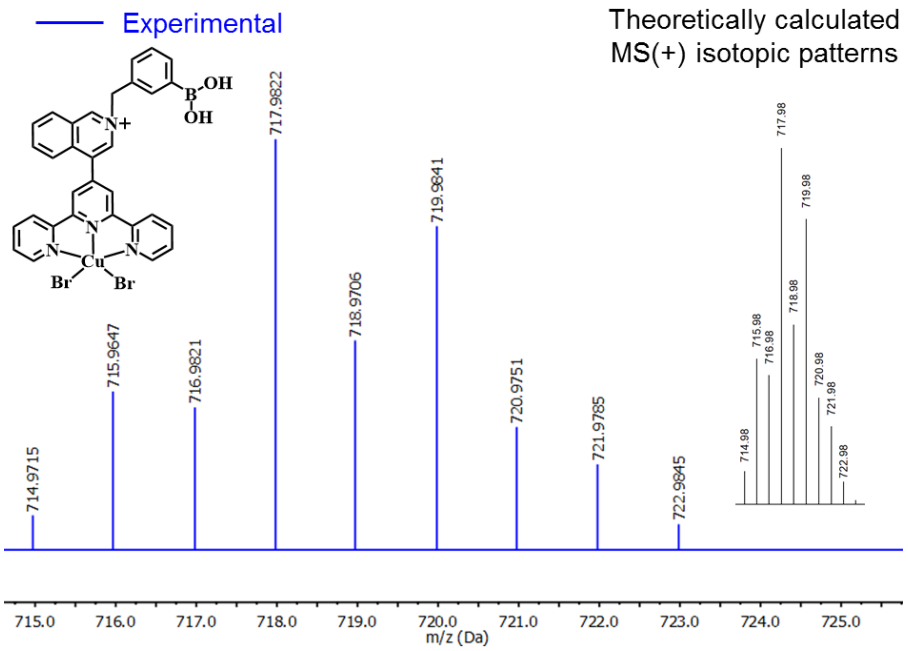

Fig. S7 High-resolution mass spectrum by a positive scan of ESI of **CuL^1** in CH_3OH. Inset: theoretically calculated MS isotopic patterns.

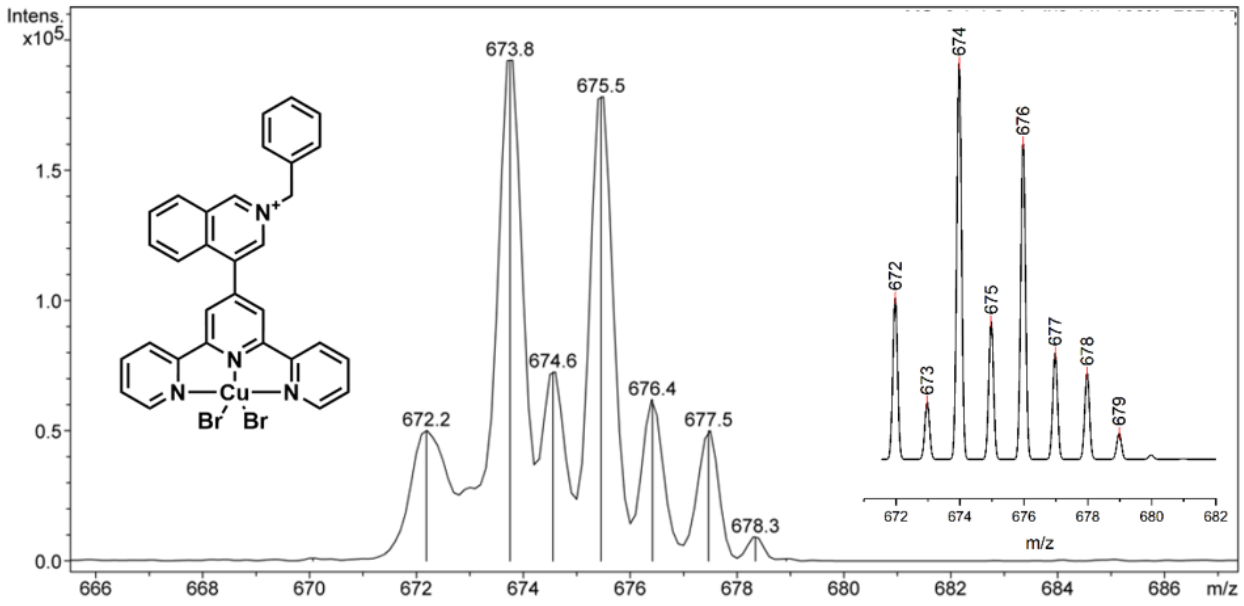

Fig. S8 Positive scan MS-ESI spectrum of **CuL^2** in CH_3OH.

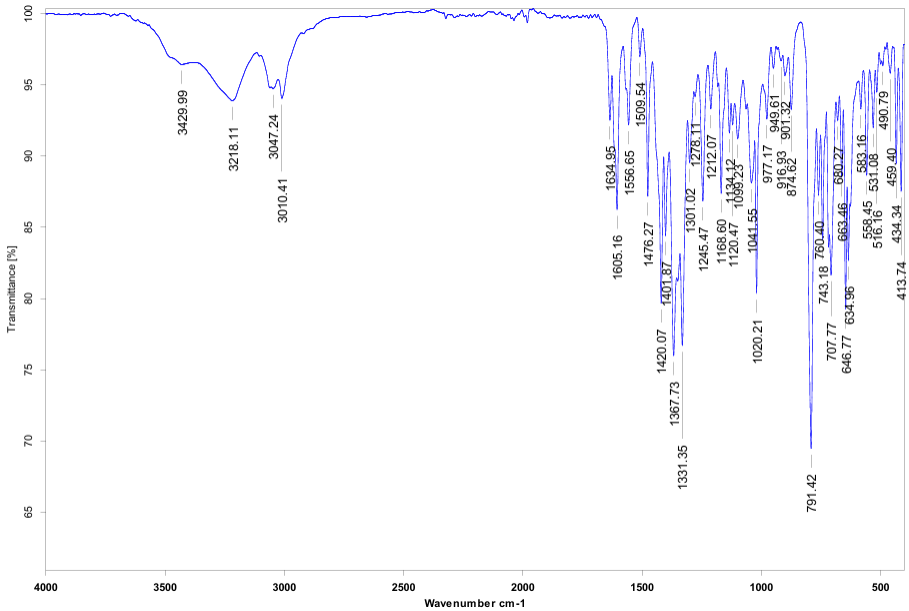

Fig. S9 IR (ATR) spectrum of **CuL^1**.

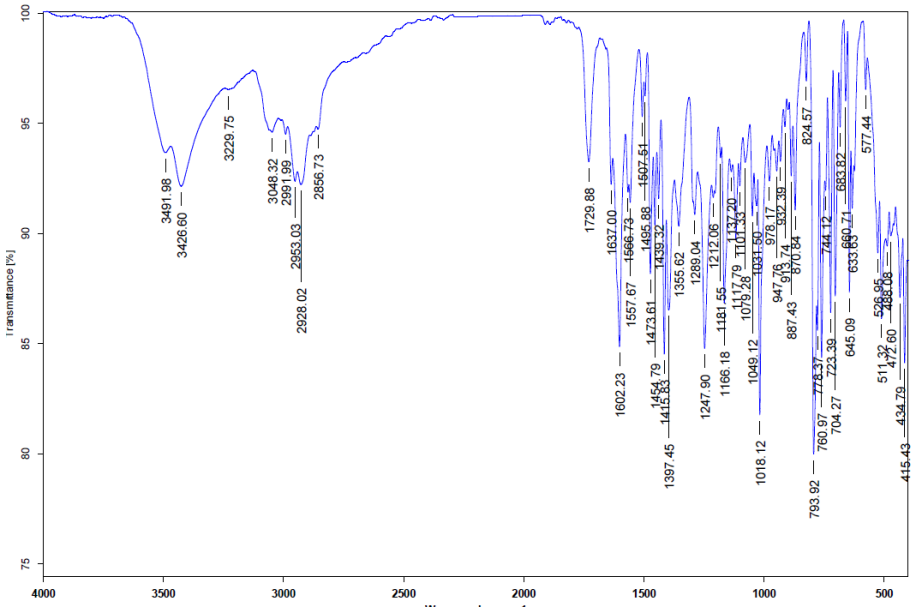

Fig. S10 IR (ATR) spectrum of **CuL^2**.

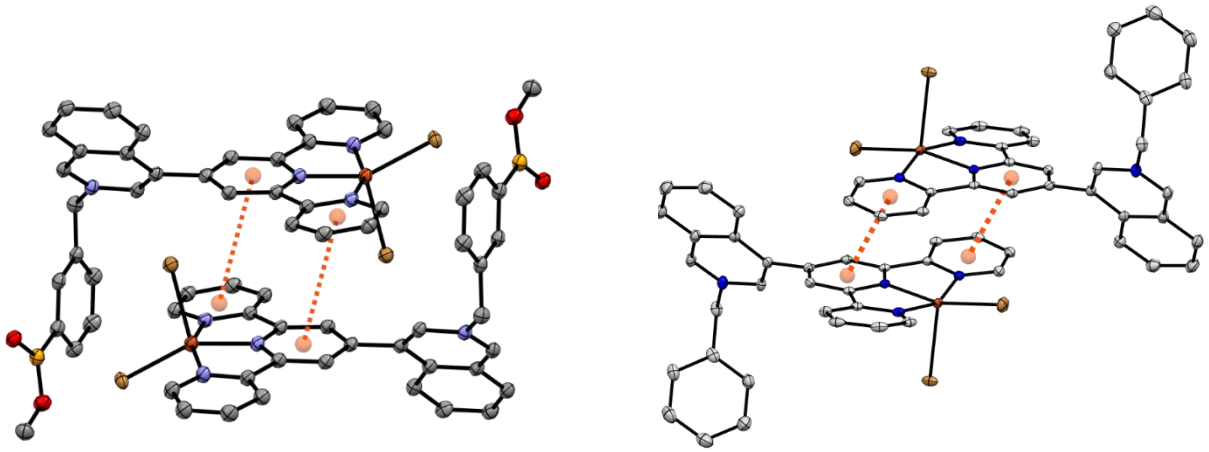

CuL^1 **CuL^2**

Fig. S11 Crystal packing ORTEP perspectives of complexes **CuL^1** and **CuL^2**. The intermolecular π···π distances (orange lines, 3.897(4) Å) for **CuL^1** and (3.836(3) Å – 3.841(5) Å) for **CuL^2** were measured between the planes of the metallated terpy-fragments.

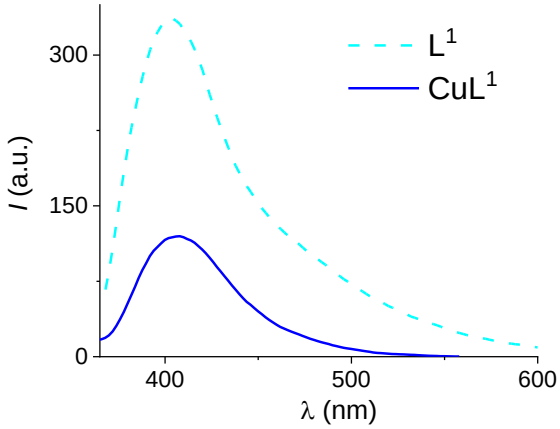

Fig. S12 Fluorescence emission spectra (10 μM, λ_{ex}= 330 nm) of **L^1** and **CuL^1** in buffered (10 mM MOPS) water at pH= 7.4.

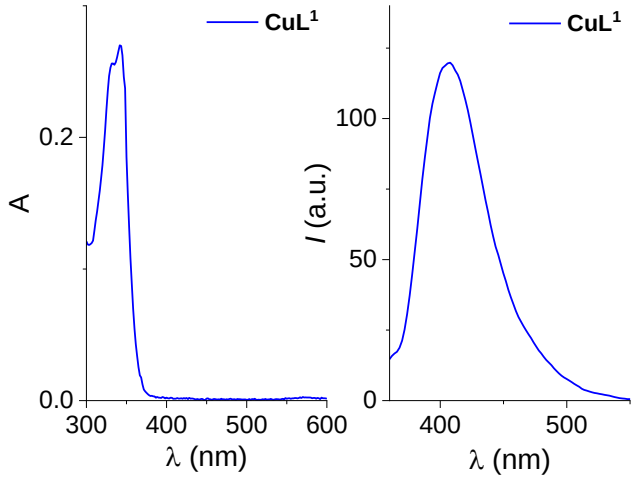

Fig. S13 Absorption (20 μM) and fluorescence emission spectra (10 μM, λ_{ex}= 330 nm) of **CuL^1** in buffered water at pH= 7.4.

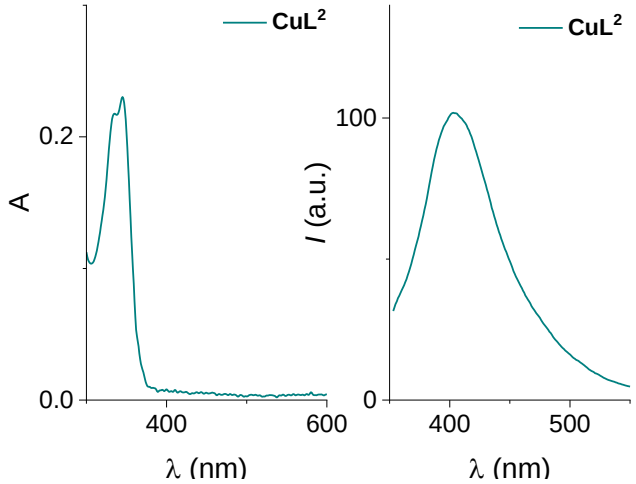

Fig. S14 Absorption (20 μM) and fluorescence emission spectra (10 μM, λ_{ex}= 330 nm) of **CuL^2** in buffered water at pH= 7.4.

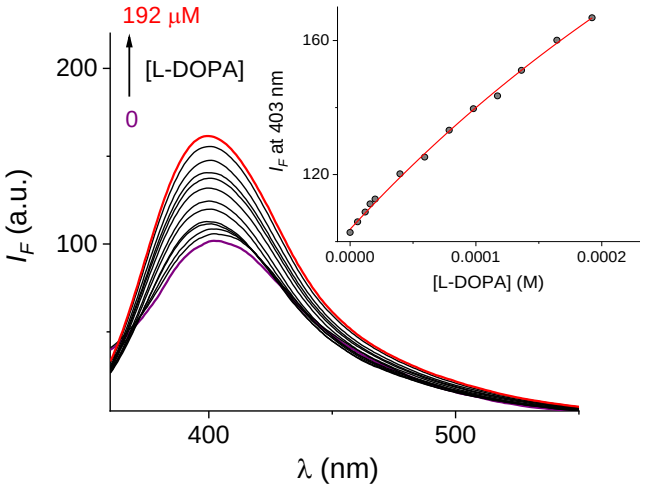

Fig. S15 Changes of emission spectra (λ_{ex}= 330 nm) of buffered (10 mM MOPS pH= 7.4, 20 mM NaCl) aqueous solutions of **CuL²** (10 μM) upon the addition of increasing amounts of Levodopa at 25 °C. Inset: Curve-fitting analysis of the fluorescence emission change at 403 nm. The solid line was obtained by fitting the experimental data to 1:1 model.